Coherent GFSK Receiver on MIMO Frequency Selective Channels

Kazuki Yoshida, Yasunori Iwanami
Dept. of Electrical and Mechnical Engineering
Nagoya Institute of Technology
Nagoya, Japan
28413188@stn.nitech.ac.jp, iwanami@nitech.ac.jp

***Abstract*— GFSK (Gaussian-filtered Frequency Shift Keying) signal has a constant envelope and is suited to power efficient nonlinear amplification. However, the application of GFSK signal to spectrally efficient and reliable MIMO (Multiple Input Multiple Output) communication schemes has not been so popular up to now. Maybe this comes from the fact that the signal processing for spatially multiplexed MIMO signal is usually done using linear matrix algebra and the application of linear signal processing techniques to nonlinear digital FM signal such as GFSK is difficult. In this paper, we study the coherent detection of GFSK signal based on MLD (Maximum Likelihood Detection) approach on MIMO frequency selective channels. In the proposed receiver, the receive replica signal which is frequency and phase synchronized is generated and the signal distance between the receive signal and the receive replica signal is minimized. By extending the observation length of receive signal, we further improved the BER characteristics. We also reduced the complexity of MLD by using the SE (Schnorr Euchner) algorithm of Sphere Decoding to obtain ML (Maximum Likelihood) solution.**

Keywords*— *MIMO, GFSK, frequency selective fading, ISI canceller, MLD, Sphere Decoding, SE algorithm

I. INTRODUCTION

GFSK signal has a constant envelope property and is appropriate to be amplified by nonlinear amplifier with high power efficiency. Due to the increasing demand of high data rate and reliable data transmission, MIMO schemes with multiple transmit and receive antennas become quite popular recently. The conventional MIMO schemes process the received QAM (Quadrature Amplitude Modulation) signals using linear matrix calculation. However it has been difficult to apply the linear equalizer to the nonlinearly modulated GFSK signal, and the equalization of GFSK signal at the receiver side has been difficult especially when it is subjected to frequency selective channels. Accordingly there was almost no research on MIMO GFSK signaling on frequency selective channels. We developed the coherent detection scheme of MFSK (M-ary FSK) using ISI (Inter-Symbol Interference) canceller and MLD in [1],[2]. In that scheme, by generating the receive replicas using already detected symbols, the ISI components caused by the past transmit symbols were cancelled by ISI canceller. Also, the ISI due to the future transmit symbols and the IAI (Inter-Antenna Interference) of MIMO spatial multiplexing were removed by MLD. In addition, zero padding is employed to circumvent the IBI (Inter Block Interference). As the GFSK signal is one of CPM (Continuous Phase Modulation) signals [3], the BER characteristics are further improved by enlarging the observation length of the received CPFSK (Continuous Phase FSK) signal [4]. In this paper, we developed a coherent MIMO GFSK receiver and improved the BER characteristics through enlarging the observation length of received signal. Moreover, we adopted the SE (Schnorr-Euchner) algorithm [5],[6] of Sphere Decoding to suppress the exponential increase of the complexity of MLD especially when the observation length is expanded. By adopting the SE algorithm, we can find the same ML solution as the MLD with far less complexity.

This paper is organized as follows. In Section II, we show some of GFSK waveforms. In Section III, the coherent MIMO GFSK receiver using ISI canceller and MLD is introduced. In Section IV, the Sphere Decoding SE algorithm with ML solution is described. In Section V, the BER characteristics of coherent MIMO GFSK receiver are simulated. We also show the improvement of BER obtained by expanding the observation length. The paper concludes with Section VI.

II. GFSK WAVEFORMS

For the binary input data sequence (+1,-1,-1,+1) having 4 symbol length, Gaussian low pass filtered waveforms are shown in Fig.1. We know when the cut-off frequency of Gaussian LPF is $f_b = 0.3/T$, it needs total 6 symbol length to transmit 4 data symbols. This is because the impulse response of Gaussian LPF spreads over $2T$. Hence GFSK is referred to as partial response signaling [3]. For any data symbol length other than 4, the total symbol length of GFSK with $f_b = 0.3/T$ always needs additional 2 vestigial symbols for terminating the response of Gaussian LPF. This becomes the overhead when

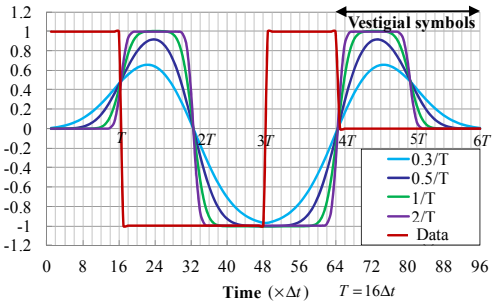

Fig. 1. GFSK (G2FSK) waveforms when the cut-off frequency of Gaussian LPF varies.

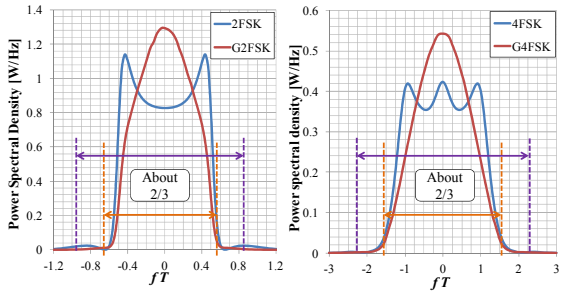

Fig. 2. Comparison of power spectral densities between GFSK and FSK with modulation index h=0.715.

the data symbol length is small. But when the data symbol length is large, this overhead length of 2 vestigial symbols becomes almost negligible. In Fig.2, we show the power spectral densities of 2FSK (binary continuous phase FSK), G2FSK (binary GFSK), 4FSK and G4FSK. When G2FSK is employed instead of 2FSK, the transmission bandwidth which contains 99% transmit power can be reduced almost by 2/3. The same observation holds between 4FSK and G4FSK. Hence, GFSK is said to be bandwidth-efficient modulation scheme.

III. Coherent GFSK Demodulator Using ISI Canceller and MLD on MIMO Frequency Selective Channels

In Fig.3, we show the block diagram of transmitter and receiver of coherent MIMO GFSK demodulation scheme using ISI canceller and MLD. At the transmitter side, after the GFSK modulated data symbols, zero symbols having the length of $N_G T$ shown in Fig.4 are inserted (Zero Padding; ZP). By using ZP, the IBI caused by multipath delayed waves between the successive blocks is prevented. Accordingly, the ZP length of $N_G T$ must be longer than the maximum delay time of delayed waves. The initial phase of the head symbol in the transmit block in Fig.4 is always set to zero. This phase reset is needed

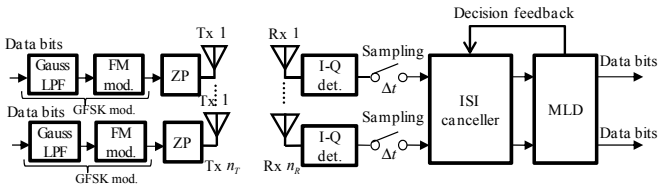

Fig.3. Transmitter and receiver configuration of MIMO GFSK with coherent demodulation using ISI canceller and MLD

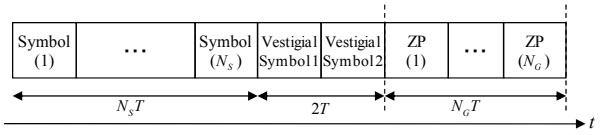

Fig.4. Transmit block structure in GFSK transmission

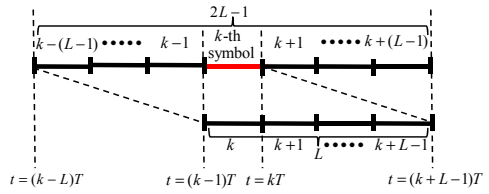

Fig.5. Search of transmit symbol sequence for detecting k-th symbol

to phase-synchronize the candidate replica signal generated at the receiver with the receive signal in coherent GFSK demodulation. At the receiver side, using I-Q (Inphase-Quadrature) detection, the complex baseband receive signal is obtained. By sampling the complex baseband signal at the rate of $2c$ samples per one symbol ($T = 2c\Delta t$), we get the discrete time signal with the sampling interval of Δt. The sampling interval Δt is taken so as to satisfy the sampling theorem. The sampled discrete time signal is then fed to the ISI canceller and finally MLD is made.

We consider the case in which the maximum delay time of the channel is $l\Delta t$ with $l\Delta t \le (L-1)T$ where l and L are integer numbers and $(L-1)$ means the number of data symbols influenced by the delayed wave. Due to the multipath delay, the k-th transmit symbol during $(k-1)T \le t < kT$ in Fig.5 spreads over the duration of $(k-1)T \le t < (k+L-1)T$ at the receiver. On the other hand, the receive symbols over $(k-1)T \le t < (k+L-1)T$ are affected by the transmit symbols during $(k-L)T \le t < (k+L-1)T$, i.e., $(2L-1)$ transmit symbols. Accordingly, to determine the k-th transmit symbol during $(k-1)T \le t < kT$, we have to observe total L receive symbols affected by $(2L-1)$ transmit symbols. To generate all the receive replicas in MLD search caused by the $(2L-1)$ transmit symbol length, it requires $M^{(2L-1)n_T}$ times calculation where M denotes the modulation level of GFSK and n_T is the number of transmit antennas. When L and n_T are large, this exponential increase of $M^{(2L-1)n_T}$ causes a problem of complexity. To reduce the number of searches over $(2L-1)$ transmit symbols in MLD, we employ the ISI canceller to cancel the ISI components caused by the transmit symbols over the past duration $(k-L)T \le t < (k-1)T$ already detected at the receiver. This makes the MLD search over L transmit symbols during $(k-1)T \le t < (k+L-1)T$ and reduce the number of MLD search to M^{Ln_T}. When the erroneous detection happens in somewhere in the block, the error propagation occurs after the erroneous symbol due to the wrong ISI cancellation. But the error propagation is obviously limited within a transmit block.

We again summarize the idea to detect the k-th symbol in Fig.5. To detect the k-th transmit symbol, we need the total L receive symbols over $k \sim k+L-1$ symbol duration. But those L receive symbols are affected by $(2L-1)$ transmit symbols over $k-(L-1)$ to $k+(L-1)$ symbol duration. Therefore, to detect the k-th symbol based on the MLD, we need to check all the transmit sequence over $k-(L-1)$ to $k+(L-1)$ transmit symbol duration. This needs $M^{(2L-1)n_T}$ searches as mentioned above. However, as the past transmit symbols over $k-(L-1) \sim (k-1)$ symbol duration have already been detected at the receiver, we can make use of those detected transmit symbols for the candidate symbols in the MLD search procedure. Hence, we can replace the past transmit symbols over $k-(L-1)$ to $(k-1)$ by the already detected results. This reduces the MLD search duration to $k \sim k+(L-1)$, i.e., L symbol length. This procedure is a kind of decision feedback and is illustrated in Fig.3. As the MLD search involves subtracting the receive candidate symbols from the receive symbols and the receive candidate symbols over $k-(L-1)$ to $(k-1)$ duration are obtained from the already detected symbols, we call this decision feedback procedure as the ISI canceller.

The total L receive symbols over $k \sim k+(L-1)$ symbol duration are expressed as

$$\begin{pmatrix} \boldsymbol{Y}_{k+(L-1)} \\ \vdots \\ \boldsymbol{Y}_{k+l} \\ \vdots \\ \boldsymbol{Y}_{k} \end{pmatrix} = \begin{pmatrix} \boldsymbol{h}_0 & \cdots & \boldsymbol{h}_p & \cdots & \boldsymbol{h}_{J_d-1} & \boldsymbol{0} & \cdots & \cdots & \boldsymbol{0} \\ \boldsymbol{0} & \boldsymbol{h}_0 & \cdots & \boldsymbol{h}_p & \cdots & \boldsymbol{h}_{J_d-1} & \boldsymbol{0} & \cdots & \boldsymbol{0} \\ \vdots & \vdots & \vdots & \vdots & \vdots & \vdots & \vdots & \vdots & \vdots \\ \boldsymbol{0} & \cdots & \boldsymbol{0} & \boldsymbol{h}_0 & \cdots & \boldsymbol{h}_p & \cdots & \boldsymbol{h}_{J_d-1} & \boldsymbol{0} \\ \boldsymbol{0} & \cdots & \cdots & \boldsymbol{0} & \boldsymbol{h}_0 & \cdots & \boldsymbol{h}_p & \cdots & \boldsymbol{h}_{J_d-1} \end{pmatrix} \begin{pmatrix} \boldsymbol{X}_{k+(L-1)} \\ \vdots \\ \boldsymbol{X}_{k} \\ \vdots \\ \boldsymbol{X}_{k-(L-1)} \end{pmatrix} + \boldsymbol{N} \quad (1)$$

where $(\boldsymbol{X}_{k+(L-1)} \ \cdots \ \boldsymbol{X}_k \ \cdots \ \boldsymbol{X}_{k-(L-1)})^T$ are the transmit symbols over $k-(L-1) \sim k+(L-1)$ duration, the channel matrix with the elements of $\boldsymbol{h}_p$, $p=0,\cdots,J_d-1$ has the maximum delay time of $(J_d-1)\Delta t$, and $\boldsymbol{N}$ means the AWGN. In (1), the transmit symbol $\boldsymbol{X}_k$ and the receive symbol $\boldsymbol{Y}_{k+l}$ are expressed as

$$\begin{cases} \boldsymbol{X}_k = (\boldsymbol{x}_{k,2c} \ \cdots \ \boldsymbol{x}_{k,n} \ \cdots \ \boldsymbol{x}_{k,1})^T \\ \boldsymbol{Y}_{k+l} = (\boldsymbol{y}_{k+l,2c} \ \cdots \ \boldsymbol{y}_{k+l,n} \ \cdots \ \boldsymbol{y}_{k+l,1})^T \end{cases} \quad (2)$$

respectively where $\boldsymbol{x}_{k,n}$ and $\boldsymbol{y}'_{k+l,n}$ in (2) are given by

$$\begin{cases} \boldsymbol{x}_{k,n} = (x_{k,n}^{(1)} \ \cdots \ x_{k,n}^{(i)} \ \cdots \ x_{k,n}^{(n_T)})^T \\ \boldsymbol{y}_{k+l,n} = (y_{k+l,n}^{(1)} \ \cdots \ y_{k+l,n}^{(j)} \ \cdots \ y_{k+l,n}^{(n_R)})^T \end{cases} \quad (3)$$

respectively. In (3) $x_{k,n}^{(i)}$ means the n-th sample $(n=1,\cdots,2c)$ of transmit signal of k-th symbol duration from transmit antenna i and $y_{k+l,n}^{(j)}$ means the n-th sample $(n=1,\cdots,2c)$ of receive signal of $(k+l)$-th symbol duration from receive antenna j. The element $\boldsymbol{h}_p$ of channel matrix in (1) is expressed as

$$\boldsymbol{h}_p = \begin{pmatrix} h_p^{(1,1)} & \cdots & h_p^{(1,i)} & \cdots & h_p^{(1,n_T)} \\ \vdots & \cdots & \vdots & \cdots & \vdots \\ h_p^{(j,1)} & \cdots & h_p^{(j,i)} & \cdots & h_p^{(j,n_T)} \\ \vdots & \cdots & \vdots & \cdots & \vdots \\ h_p^{(n_R,1)} & \cdots & h_p^{(n_R,i)} & \cdots & h_p^{(n_R,n_T)} \end{pmatrix} \quad (4)$$

where the element $h_p^{(j,i)}$ in (4) means the complex channel gain with the delay time of $p\Delta t$ from transmit antenna i to receive antenna j.

The channel delay profile between transmit antenna i and receive antenna j is shown in Fig.6.

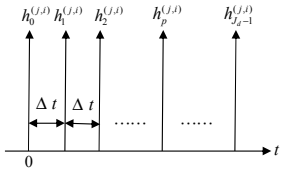

Fig.6. Delay profile between transmit i and receive antenna j

In order to detect the k-th transmit symbol, the MLD over $(2L-1)$ transmit symbol duration is executed based on the following MLD criteria

$$\boldsymbol{X}_k = \underset{\boldsymbol{X}_{k-(L-1)},\cdots,\boldsymbol{X}_{k+(L-1)}}{\arg\min} \left\| (\boldsymbol{Y}_{k+(L-1)},\cdots,\boldsymbol{Y}_k)^T - (\boldsymbol{Y}'_{k+(L-1)},\cdots,\boldsymbol{Y}'_k)^T \right\|^2 \quad (5)$$

where $(\boldsymbol{Y}'_{k+(L-1)},\cdots,\boldsymbol{Y}'_k)$ denotes the candidate receive replica sequence generated at the receiver which correspond to the receive sequence in the absence of AWGN. In (5), however, $\boldsymbol{X}_{k-(L-1)},\cdots,\boldsymbol{X}_{k-1}$ are already detected results and can be fixed. Accordingly, instead of (5), the MLD search over $\boldsymbol{X}_k,\cdots,\boldsymbol{X}_{k+(L-1)}$ can be done by the criteria as follows.

$$\boldsymbol{X}_k = \underset{\boldsymbol{X}_k,\cdots,\boldsymbol{X}_{k+(L-1)}}{\arg\min} \left\| (\boldsymbol{Y}_{k+(L-1)},\cdots,\boldsymbol{Y}_k)^T - (\boldsymbol{Y}'_{k+(L-1)},\cdots,\boldsymbol{Y}'_k)^T \right\|^2 \quad (6)$$

We have named the operation in (6) as {ISI canceller + MLD}.

IV. Application of Sphere Decoding SE Algorithm

The SE algorithm [5], [6], one of the Sphere Decoding algorithms, achieves the ML solution like in MLD, while greatly reducing the complexity compared with MLD. We illustrate the SE algorithm briefly in Fig.7. On the MLD tree structure in Fig.7, the SE algorithm firstly searches the path in depth direction (in time axis direction) using M-algorithm [7]. The quasi-optimum path obtained through M-algorithm is depicted as red-colored {2}{4}{6}{7}{9}{10} in Fig.7. The quasi-ML solution of transmit sequence is called Babai point. We set the path metric corresponding to Babai point to C^2 (initial squared radius). The tree search is again done to the depth direction in Fig.7 to satisfy the accumulated path metric less than C^2. If the accumulated path metric exceeds C^2 in the tree search, there is no need to find the subsequent diverging paths following that branch. This leads to save the extra tree searching procedure. If the accumulated path metric does not exceed C^2 up to the bottom of tree, then C^2 is regarded as the new initial squared radius. Finally, the entire tree search results in finding the ML solution with reduced complexity.

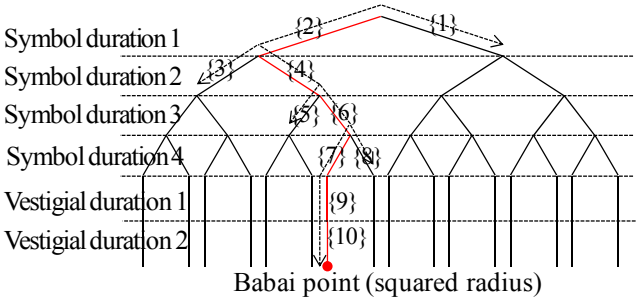

Fig.7. Tree structure of Sphere Decoding SE algorithm (G2FSK, number of transmit and receive antennas; $n_T = n_R = 1$, L=4 corresponding to Fig.1)

V. BER Characteristics of Coherent GFSK Receiver on MIMO Frequency Selective Channels

Computer simulation is done based on the block diagram of Fig.3 for the coherent GFSK receiver using ISI canceller with MLD or SE algorithm on MIMO frequency selective channels. We also compare the BER of GFSK with the one of FSK. The simulation condition is shown in Table I and Fortran was used as a compiler language.

Fig.8 shows the BER characteristics of {ISI canceller + MLD} and {ISI canceller + Sphere Decoding SE algorithm} for 2×2 G4FSK and 4FSK. From Fig.8, we know there is no BER difference between {ISI canceller + MLD} and {ISI canceller + Sphere Decoding SE algorithm}.

TABLE I. Simulation Condition for Coherent MIMO GFSK Receiver

Modulation	G4FSK
Modulation index	h=0.715
Number of transmit and receive antenna	2×2
Channel model between each Tx and Rx antenna	Quasi-static Rayleigh fading with equal power 16 delay paths
Equalization and signal separation at receiver	ISI canceller) + (MLD or Sphere Decoding SE algorithm)
Number of samples in a symbol	T=2c Δt , 2c=16
Symbol duration	T
Interval of delay waves	$T/16$ (= Δt)
Maximum delay time	$15T/16 < T$
ZP length	$1 \cdot T$
Transmit block length in Fig.4	$N_s T + 2T + N_G T = 16T + 2T + 1T = 19T$

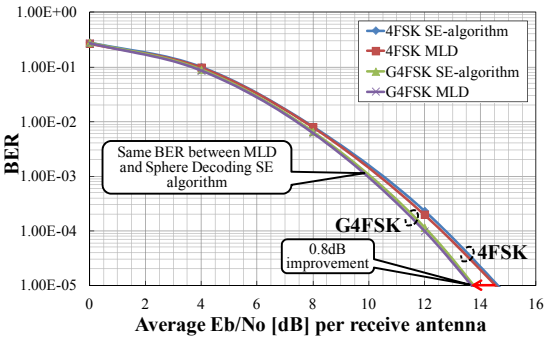

Fig.8. BER characteristics of coherent G4FSK receiver on MIMO (2×2) frequency selective channel

We also find that G4FSK shows the better BER than 4FSK by 0.8 dB at BER=10^{-5} .

The receiver with {ISI canceller + MLD} makes the MLD search over L symbol duration $k \sim k+(L-1)$ as in (6) to determine the transmit signal $\boldsymbol{X}_k$. However, for the coherent detection of CPFSK, the BER of the 1st symbol in the transmit block is further improved by a few dB through the longer observation length of $4T \sim 5T$ rather than one symbol duration T [4]. Therefore, we extended the observation length in MLD in (6) from LT to $N_wT=(L+w)T,\ (w=0,1,2,\cdots)$ and aim to improve the BER characteristics, where $w=0$ corresponds to the usual receiver in (6). Extending the symbol duration N_wT for MLD causes the increasing number of replica search growing exponentially as $M^{(L+w)\cdot n_T}$. However, we solve this problem by using the Sphere Decoding SE algorithm. We made the simulation when the symbol length of MLD is extended to N_wT . The simulation condition is the same as in Table I except for the extended MLD length, i.e., $N_wT=(L+w)T,\ (L=2,\ w=0,1,2,3)$. The BER characteristics are shown in Fig.9. By expanding the observation length of MLD from $N_wT=2T\,(w=0)$ to $N_wT=5T\,(w=3)$, we get the BER improvement about 2.3 dB at BER=10^{-5} .

In Fig.10, we also show the number of branch metric calculation when using the Sphere Decoding SE algorithm. From Fig.10, we see that for high E_b/N_0 region larger than 8 dB, the number of branch metric calculation is sufficiently reduced by using the Sphere Decoding SE algorithm which attains the same BER as MLD.

VI. Conclusions

In this paper, we discussed the coherent detection of GFSK signal on MIMO frequency selective channels. By generating the frequency and phase synchronized replica signal at the receiver, the transmit signal which minimizes the squared distance between the receive signal and the receive replica signal is determined by the MLD search. In the MLD search, the ISI components due to the past transmit symbols are cancelled by using already detected results. The exponentially growing complexity of MLD is greatly reduced by the Sphere Decoding SE algorithm which obtains the same ML solution as MLD. By utilizing the phase memory effect of GFSK and extending the observation length of MLD at the receiver, we achieved further BER improvement while reducing the complexity with the Sphere Decoding SE algorithm. As a result, G4FSK shows the better BER than 4FSK by 0.8 dB at BER=10^{-5} with less

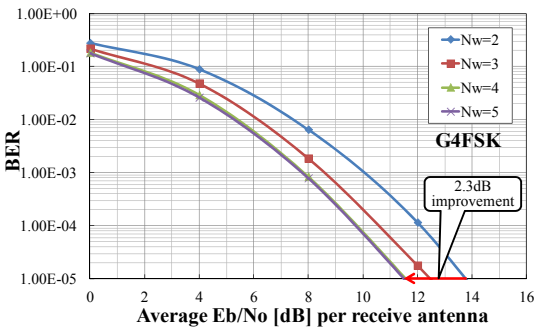

Fig.9. BER characteristics when the observation length is extended.

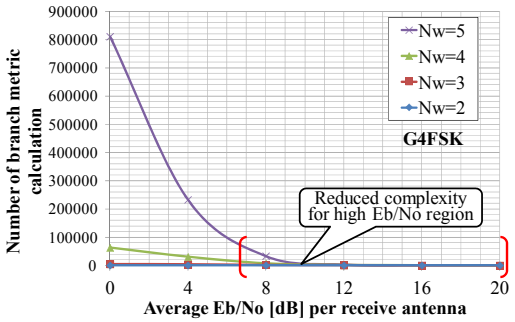

Fig.10. Number of branch metric calculation in Sphere Decoding SE algorithm when the observation length is extended.

bandwidth of 2/3. Furthermore additional 2.3 dB improvement at BER=10^{-5} is possible by expanding the observation length at the receiver. One of the applications of the proposed MIMO coherent GFSK schemes might be the power efficient short range wireless communications with high speed. As future studies, the coherent detection of power and bandwidth-efficient CPM signals other than GFSK and FSK will be discussed on MIMO frequency selective channels.

Acknowledgment

This study is supported by the Grants-in-Aid for Scientific Research JP15K06059 of the Japan Society for the Promotion of Science and the Sharp Corporation. The authors also thank Mr. Rio Abe for his contributions.

References

[1] Y. Iwanami and K. Nakayama, “MLD-based MFSK Demodulation on MIMO Frequency Selective Fading Channel,” ICWMC2011, pp.30-35, ISBN 978-1-61208-140-3, June 2011.

[2] R. Abe and Y. Iwanami, “Coherent MFSK detection on MIMO frequency selective channels,” IEEE ICDIPC2015, pp.77-82, Oct. 2015.

[3] J.B. Anderson, T. Aulin, C-E. Sundberg, “Digital phase modulation,” Plenum press, New York and London, 1986.

[4] T. A. Schonhoff, “Symbol error probabilities for M-ary CPFSK: coherent and noncoherent detection,” IEEE Trans. on Commun., vol.24, no.6, pp.644-652, June 1976.

[5] Z. Guo, P. Nilsson, “Reduced Complexity Schnorr-Euchner Decoding Algorithms for MIMO systems,” IEEE communication letters, vol.8, no.5, pp.286-288, May 2004.

[6] B. Shim, I. Kang, “Sphere Decoding with a probabilistic tree pruning,” IEEE transactions on signal processing, vol.56, No.10, pp.4867-4878, Oct. 2008.

[7] J. B. Anderson, “Limited search trellis decoding of convolutional codes,” IEEE Trans. Inform. Theory, vol. 35, No.5, pp.944-955, Sept. 1989.